



Cobalt(II) complexes with bis(*N*-imidazolyl/benzimidazolyl) pyridazine: Structures, photoluminescent and photocatalytic properties



Jin-Ping Li, Jian-Zhong Fan, Duo-Zhi Wang*

Key Laboratory of Material and Technology for Clean Energy, Ministry of Education, Chemistry and Chemical Engineering School of Xinjiang University, Urumqi 830046, PR China

ARTICLE INFO

Article history:

Received 23 January 2016

Received in revised form

31 March 2016

Accepted 25 April 2016

Available online 30 April 2016

Keywords:

Co^{II} complexes

Crystal structure

Luminescent property

Photocatalytic activity

ABSTRACT

Six new Co^{II} complexes [Co(L¹)₄(OH)₂] (1), {[Co(L¹)(H₂O)₄] · 2ClO₄]_∞ (2), {[Co(L¹)(H₂O)₄] · SiF₆]_∞ (3), {[Co(L¹)₃] · 2ClO₄]_∞ (4), [Co(L²)Cl₂]_∞ (5) and {[Co(L²)₂] · SiF₆]_∞ (6) [L¹ = 3,6-bis(*N*-imidazolyl) pyridazine, L² = 3,6-bis(*N*-benzimidazolyl) pyridazine] have been synthesized and characterized by elemental analysis, IR spectra and single crystal X-ray diffraction. Complex **1** has a mononuclear structure, while complexes **2** and **3** have 1-D chain structures. Considering the Co^{II} centers were linked by the L¹ ligands, the 3-D framework of complex **4** can be rationalized to be a {412.63} 6-c topological net with the stoichiometry uninodal net. **5** reveals a coordination 1-D zigzag chain structure consisting of a neutral chain [Co(L²)Cl₂]_n with the Co^{II} centers. Complex **6** has a rhombohedral grid with a (4, 4) topology. The TGA property, fluorescent property and photocatalytic activity of complexes **1–6** have been investigated and discussed.

© 2016 Elsevier Inc. All rights reserved.

1. Introduction

In recent years, the rational design and assembly of solid coordination network (SCF) have been an attractive research field in supramolecular chemistry and coordination chemistry owing to their fascinating structural diversities as well as their potential applications in many fields, such as catalysis, sensing, photovoltaics, ion exchange, microelectronics, nonlinear optics and so on [1–6]. The construction of solid coordination network (SCF) with desired structures and specific properties still remains a far-reaching challenge because there are so many factors influencing the formation and structure of the complexes [7,8], especially, the structure of organic ligands and the coordination modes of metal ions [9]. An effective and facile approach for the synthesis of such complexes with specific structures and properties is carried out by the utilization of well-designed organic ligands and metal ions [10]. Among the various organic ligands, the ligands of imidazole derivatives have received considerable attention because these compounds have a variety of pharmacological activities like fungicides or anti-helminthics [11]. The complexes of bis(imidazole/benzimidazole) ligands containing two imidazole rings capable of acting as hydrogen bond donors are linked into high-dimensional

supramolecular networks [12]. A large number of metal coordination compounds of imidazole and benzimidazole with luminescent properties and novel topologies have been reported [13].

Furthermore, from the standpoint of property investigation, Co^{II} metal with d⁷ electronic configuration is often employed in crystal engineering owing to excellent electrochemical property [14], magnetic property [15], photoluminescent property [16] when it is coordinated to organic ligands. However, the reports of Co^{II} metal complexes about photocatalysts are still very limited [17].

Pyridazines are well established as potential bridging units in binuclear complexes since they are capable of spanning two metal ions via their two N atoms [18,19]. 3,6-bis(*N*-imidazolyl) pyridazine as a kind of heterocyclic ligand has been reported, and Jin and his cooperators [20,21] reported a series of chlorocadmate complexes with imidazole derivatives under strong acidic condition. But in their articles, the Cd^{II} ions of all compounds were tetrahedrally coordinated by Cl[−], while 3,6-bis(*N*-imidazolyl) pyridazine ligand has not taken part in coordination. In this work, we focus our attention on the coordination chemistry of ligands containing pyridazine, two structurally related neutral ligands, 3,6-bis(*N*-imidazolyl) pyridazine (L¹) and 3,6-bis(*N*-benzimidazolyl) pyridazine (L²) (Chart 1) as an extension of our work, and six Co^{II} metal-organic complexes were synthesized and structurally characterized. In these Co^{II} complexes, because of the difference of

* Corresponding author.

E-mail address: wangdz@xju.edu.cn (D.-Z. Wang).

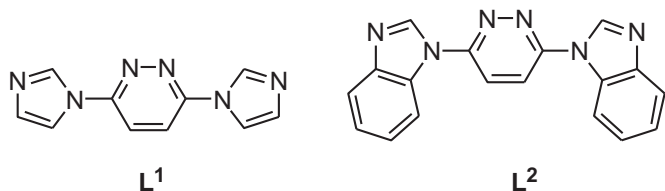


Chart 1. The ligands **L**¹ and **L**² studied in this work.

L¹ and **L**² ligands, the Co^{II} centers of complexes **1–4** adopted octahedral coordination spheres, while they adopted tetrahedral coordination sphere in complexes **5** and **6**. Moreover, the fluorescent property and photocatalytic activity of complexes **1–6** have been investigated and discussed.

2. Experimental section

2.1. Materials and general methods

All the other reagents used for the syntheses were commercially available and employed without further purification. Imidazole, benzimidazole, and 3,6-dichloropyridazine were purchased from J&K Scientific LTD, whose purities are 99%, 98% and 97%, respectively. Elemental analysis of C, H and N were determined with a Thermo Flash EA 1112-NCHS-O analyzer. IR spectra were measured via KBr pellets using a Bruker Equinox 55 FT-IR spectrometer. NMR data were collected using an INOVA-400 NMR spectrometer and chemical shifts are reported in δ relative to TMS. High-resolution mass spectra (HRMS) were recorded on Thermo Q-Exactive. Solid state luminescent spectra of ligands **L**¹, **L**² and complexes **1–6** were measured by Hitachi F-4500 Fluorescence Spectrophotometer with a Xe arc lamp as the light source and bandwidths of 2.5 nm at room temperature. UV–vis absorption spectra were obtained using a Hitachi UV-3010 UV–vis spectrophotometer. The X-ray powder diffraction (XRPD) was recorded on a Rigaku D/Max-2500 diffractometer at 40 kV, 100 mA for a Cu-target tube and a graphite monochromator.

2.2. Synthesis of ligands **L**¹ and **L**²

2.2.1. 3,6-bis(N-imidazolyl) pyridazine (**L**¹)

Imidazole (3.4 g, 49.9 mmol), sodium (1.2 g, 52.2 mmol) and 80 mL THF was added to a 250 mL three-necked flask. The reaction mixture was refluxed for 40 min. A solution of 3,6-dichloropyridazine (3.7 g, 24.8 mmol) in 10 mL THF was added to the mixture within 40 min. The mixture was refluxed for 4 h under N₂. The reaction mixture was poured into ice water after being cooled to room temperature. The earthy yellow solid of **L**¹ was obtained after filtering. Pure ligand **L**¹ was obtained by recrystallization from ethanol as white crystals. Yield 80%. m.p. 281–282 °C. ¹H NMR (400 MHz, DMSO-*d*₆): δ : 8.69 (s, 2 H, imidazole-2), 8.48 (s, 2 H, pyridazine), 8.11 (d, 2 H, *J*=2.4 Hz, imidazole-5), 7.23 (d, 2 H, *J*=2.4 Hz, imidazole-4); ¹³C NMR (100 MHz, DMSO-*d*₆): 151.32, 135.46, 130.72, 121.60, 116.73. HRMS: (ESI) calcd for C₁₀H₈N₆, ([M+H]⁺): 213.0805, found: 213.0875; Anal. Calcd for C₁₀H₈N₆: C, 56.60; H, 3.80; N, 39.60; Found: C, 56.75; H, 3.75; N, 39.54. IR (cm⁻¹, KBr pellets): 3176w, 3145m, 3109m, 3047m, 3018m, 2946m, 2782w, 2621w, 2526w, 2408w, 2214w, 1991w, 1903w, 1795w, 1727w, 1692w, 1645w, 1577s, 1519s, 1490s, 1459s, 1371s, 1321s, 1277s, 1237s, 1163m, 1106m, 1059m, 1031s, 962m, 903m, 861s, 823s, 766s, 749s, 645s, 613m, 507w, 487m, 421m.

2.2.2. 3,6-bis(N-benzimidazolyl) pyridazine (**L**²)

Ligand **L**² was synthesized similarly as **L**¹ by using

benzimidazole instead of imidazole. Yield 76%. m.p. 283–284 °C. ¹H NMR (400 MHz, DMSO-*d*₆): δ : 9.130 (s, 2 H, imidazole-2), 8.653 (s, 2 H, pyridazine), 7.388–8.384 (m, 8 H, benzene); ¹³C NMR (100 MHz, DMSO-*d*₆): 152.30, 144.34, 142.26, 131.68, 124.53, 123.71, 122.51, 120.09, 114.64; HRMS: (ESI) calcd for C₁₈H₁₂N₆, ([M+H]⁺): 313.1196, found: 313.1187; Anal. Calcd for C₁₈H₁₂N₆ (%): C, 69.21; H, 3.87; N, 26.91; Found (%): C, 69.34; H, 3.56; N, 27.41. IR (KBr, cm⁻¹): 3082m, 3058m, 2924w, 2854w, 2773w, 2371w, 1921w, 1783w, 1739w, 1669w, 1609m, 1590m, 1558s, 1497s, 1459s, 1359m, 1338m, 1308m, 1279m, 1238m, 1190s, 1163m, 1138m, 1035m, 992m, 979m, 962m, 939m, 884m, 830m, 769s, 753s, 732s, 644m, 623m, 575m, 538m, 486m, 427m.

2.3. Synthesis of complexes **1–6**

2.3.1. [Co(**L**¹)₄(OH)₂] (1)

A mixture of Co(NO₃)₂·6H₂O (87 mg, 0.3 mmol) and **L**¹ (63 mg, 0.3 mmol) and 5 mL water, was placed in a Teflon-lined stainless steel vessel (25 mL) and heated to 140 °C for 3 days, then cooled to room temperature at a rate of 10 °C·h⁻¹. The red block crystals of **1** were obtained (ca. 30% yield based on **L**¹). Anal. Calcd for C₄₀H₃₄CoN₂₄O₂: C, 51.01; H, 3.64; N, 35.69. Found: C, 50.85; H, 3.60; N, 35.60. IR (cm⁻¹, KBr pellets): 3386m, 3114m, 2525w, 2416w, 2212w, 2080w, 1995w, 1911w, 1870w, 1806w, 1579m, 1522m, 1481s, 1377s, 1318s, 1241m, 1148m, 1099m, 1065m, 1032m, 967m, 931m, 917m, 838m, 737m, 652m, 615m, 492m, 419m.

2.3.2. {[Co(**L**¹)(H₂O)₄]·2ClO₄]_∞ (2)

The pink block crystals of **2** suitable for X-ray analysis were obtained by the similar method described for **1**, except for using Co(ClO₄)₂·6H₂O instead of Co(NO₃)₂·6H₂O (ca. 35% yield based on **L**¹). Anal. Calcd for C₁₀H₁₆Cl₂CoN₆O₁₂: C, 24.86; H, 3.34; N, 17.39. Found: C, 24.58; H, 3.51; N, 17.45. IR (cm⁻¹, KBr pellets): 3368m, 3178m, 3131m, 2577w, 2385w, 2025w, 1925w, 1806w, 1646m, 1582m, 1497s, 1455s, 1301s, 1256m, 1074s, 1048s, 967m, 927m, 821m, 769m, 643m, 615m, 531m, 496m, 446m.

2.3.3. {[Co(**L**¹)(H₂O)₄]·SiF₆]_∞ (3)

A mixture of CoSiF₆·6H₂O (15 mg, 0.05 mmol) and **L**¹ (10 mg, 0.05 mmol) in water (8 mL) and ethanol (8 mL) was refluxed for 3 h. The red block crystals of **3** were formed after several days with the evaporation of the filtrate (ca. 45% yield based on **L**¹). Anal. Calcd for C₁₀H₁₆CoF₆N₆O₄Si: C, 24.75; H, 3.32; N, 17.32. Found: C, 25.14; H, 3.35; N, 17.60. IR (cm⁻¹, KBr pellets): 3409s, 3173m, 3155m, 3146m, 3064m, 2361w, 1919w, 1657m, 1574m, 1534s, 1489s, 1463s, 1373m, 1326s, 1293m, 1254m, 1155m, 1109m, 1076m, 1053m, 1038m, 970m, 937m, 868m, 844m, 761m, 716s, 649m, 617m.

2.3.4. {[Co(**L**¹)₃]·2ClO₄]_∞ (4)

A buffer layer of acetonitrile/chloroform (10 mL, 1: 1) was carefully layered over a chloroform solution (3 mL) of **L**¹ (10 mg, 0.05 mmol). Then a solution of Co(ClO₄)₂·6H₂O (22 mg, 0.05 mmol) in acetonitrile (3 mL) was layered on the buffer layer. The system was left for about two weeks at room temperature, and pink block crystals of **4** were obtained. (ca. 40% yield based on **L**¹). Anal. Calcd for C₃₀H₂₄N₁₈Cl₂O₈Co: C, 40.28; H, 2.70; N, 28.19. Found: C, 40.39; H, 2.68; N, 28.17. IR (cm⁻¹, KBr pellets): 3479m, 3137m, 3083m, 3024m, 2603w, 2415w, 2213w, 2013w, 1909w, 1806w, 1580m, 1490s, 1452s, 1370m, 1324m, 1305s, 1236m, 1095s, 1036m, 969s, 930m, 835m, 749m, 654m, 620m, 492m.

2.3.5. [Co(**L**²)Cl₂]_∞ (5)

A mixture of CoCl₂·6H₂O (71 mg, 0.3 mmol) and **L**² (93 mg, 0.3 mmol) and 6 mL ethanol, was placed in a Teflon-lined stainless steel vessel (25 mL) and heated to 140 °C for 2 days, then cooled to room temperature at a rate of 10 °C·h⁻¹. The blue block crystals of

5 were obtained (ca. 35% yield based on **L**²). Anal. Calcd for C₁₈H₁₂Cl₂CoN₆: C, 48.89; H, 2.74 N, 19.01. Found: C, 48.85; H, 2.71; N, 19.19. IR (cm⁻¹, KBr pellets): 3849w, 3796w, 3730w, 3668w, 3644w, 3441w, 3143m, 3100m, 3041w, 2839w, 2546w, 1957w, 1920w, 1838w, 1802w, 1704w, 1652w, 1607m, 1589m, 1564m, 1510s, 1466s, 1382m, 1320m, 1300m, 1239s, 1149m, 1036m, 1009m, 979w, 944w, 911w, 845w, 808w, 777s, 763s, 680w, 642m, 616m, 587m, 520m, 449m, 423m.

2.3.6. {[Co(L²)₂]·SiF₆]_∞ (6)

Crystals of **6** were obtained by the similar method described for **5**, except for using CoSiF₆·6H₂O instead of CoCl₂·6H₂O (ca. 25% yield based on **L**²). Anal. Calcd for C₃₆H₂₄CoF₆N₁₂Si: C, 52.37; H, 2.93; N, 20.36. Found: C, 52.45; H, 2.99; N, 20.78. IR (cm⁻¹, KBr pellets): 3487w, 3150m, 3107m, 3081m, 2978w, 2795w, 2522w, 1925w, 1790w, 1706w, 1572m, 1503s, 1479m, 1462m, 1441s, 1363m, 1310m, 1295m, 1233s, 1158m, 1129m, 1054s, 914m, 851m, 837m, 780m, 746s, 679m, 611m, 519m, 448m, 418m.

Caution! Perchlorate complexes of metal ions in the presence of organic ligands are potentially explosive. Only a small amount of material should be used and handled with care.

2.4. X-Ray crystallography

The X-ray diffraction (XRD) data of complexes **1–6** was collected on a Bruker APEX II Smart CCD diffractometer at 293(2) K with Mo-K α radiation ($\lambda=0.71073$ Å) by ω - ϕ scan modescan mode. Semi-empirical absorption corrections were applied to the data using SADABS program. The program SAINT [22] was used for integration of the diffraction profiles. The structures were solved by direct methods using the SHELXS program of the SHELXTL package and refined by full-matrix least-squares methods with SHELXL [23]. Metal atoms in each complex were located from the E-maps and other non-hydrogen atoms were located in successive difference Fourier syntheses and refined with anisotropic thermal parameters on F^2 . Hydrogen atoms of carbon were located at calculated positions and refined with fixed thermal parameters riding on their parent atoms. Experimental details for the structure determination are presented in Table 1.

3. Results and discussion

3.1. Syntheses and general characterization

In this work, our synthetic method of the ligands was different from the reported in literature [21]. The yields of ligands were higher than previous one. The structures of **L**¹ and **L**² determined by ¹H NMR, ¹³C NMR, IR, HRMS and elemental analysis. All the complexes **1–6** were air stable at room temperature. Complexes **1**, **2** and **5**, **6** were synthesized by the hydrothermal method at 140 °C without adding any base for adjusting the pH value. **3** was obtained in mixed solvent by refluxing for 3 h after being cooled and filtrated. Complex **4** was obtained in organic solvent at room temperature. Complex **1** has a mononuclear structure. Complexes **2** and **3** have 1-D chain structures. Complex **4** can be rationalized to be a {412.63} 6-c topological net. Complex **5** reveals a coordination 1-D zigzag chain. Complex **6** has a rhombohedral grid with a (4, 4) topology.

In the IR spectra of **1**, **2** and **3**, the bands of the coordinated H₂O molecules appeared at about 3300 cm⁻¹. The absorption bands at 1074 and 615 cm⁻¹ indicate the existence of the ClO₄⁻ anions in **2**, and characteristic bands of the free ClO₄⁻ anions appear at 1095 cm⁻¹ and 620 cm⁻¹ in **4**. The bands at 970 and 1054 cm⁻¹ were assigned to the free SiF₆

Table 1
Crystal data and structure refinement summary for complexes **1–6**.

	1	2	3
Formula	C ₄₀ H ₃₄ CoN ₂₄ O ₂	C ₁₀ H ₁₆ C ₁₂ CoN ₆ O ₁₂	C ₁₀ H ₁₆ CoF ₆ N ₆ O ₄ Si
Formular wt	941.86	542.12	485.24
Crystal system	Orthorhombic	Orthorhombic	Triclinic
Space group	<i>Ab</i> a2	<i>C</i> 22(1)	<i>P</i> -1
T/K	293(2)	296(2)	293(2)
<i>a</i> /Å	13.770(3)	9.1632(19)	7.635(2)
<i>b</i> /Å	13.780(3)	36.472(8)	11.179(3)
<i>c</i> /Å	27.590(5)	9.159(2)	11.545(3)
<i>a</i> /deg	90	90	102.803(7)
<i>b</i> /deg	90	90	107.065(7)
<i>g</i> /deg	90	90	106.551(7)
<i>V</i> /Å ³	5235.2(19)	3061.0(11)	851.4(4)
<i>Z</i>	4	4	2
<i>D</i> /g cm ⁻³	1.198	1.176	1.862
<i>m</i> /mm ⁻¹	0.384	0.784	1.174
<i>F</i> (000)	1948	1100	474
Measuredreflins	19,691	9418	5410
Obsd reflins	4593	2703	3016
<i>R</i> ^a / <i>wR</i> ^b	0.0696/0.1931	0.0656/0.2497	0.0871/0.2546
	4	5	6
Formula	C ₃₀ H ₂₄ Cl ₂ CoN ₁₈ O ₈	C ₁₈ H ₁₂ Cl ₂ CoN ₆	C ₃₆ H ₂₄ CoF ₆ N ₁₂ Si
Formular wt	894.50	442.17	825.69
Crystal system	Trigonal	Orthorhombic	Tetragonal
Space group	<i>R</i> -3c	<i>P</i> 2(1)2(1)2(1)	<i>P</i> 4(2)/n
T/K	293(2)	296(2)	296(2)
<i>a</i> /Å	13.851(3)	9.9546(4)	12.5740(6)
<i>b</i> /Å	13.851(3)	12.1863(6)	12.5740(6)
<i>c</i> /Å	58.358(17)	15.0008(7)	11.2126(8)
<i>a</i> /deg	90	90	90
<i>b</i> /deg	90	90	90
<i>g</i> /deg	120	90	90
<i>V</i> /Å ³	9696(4)	1819.74(14)	1772.77(17)
<i>Z</i>	6	4	2
<i>D</i> /g cm ⁻³	0.919	1.614	1.547
<i>m</i> /mm ⁻¹	0.392	1.253	0.597
<i>F</i> (000)	2729	892	838
Measuredreflins	24,854	11,898	10,340
Obsd reflins	2762	3292	1528
<i>R</i> ^a / <i>wR</i> ^b	0.0730/0.2138	0.0375/0.0943	0.0509/0.1556

$$^a R = \frac{\sum(|F_o| - |F_c|)}{\sum F_o}$$

$$^b wR = \left[\frac{\sum w(|F_o|^2 - |F_c|^2)^2}{\sum w(F_o^2)} \right]^{1/2}$$

3.2. Description of the crystal structure

3.2.1. [Co(L¹)₄(OH)₂] (1)

Single crystal X-ray diffraction analysis reveals that complex **1** crystallizes in the orthorhombic space group *Ab*a2 and crystallographic data and experimental details for structural analyses were summarized in Table 1, the selected bond distances and angles were listed in Table 1 of Supplementary 1. Complex **1** has a mononuclear structure (Fig. 1a). The complex **1** contains one Co^{II} cation, four neutral **L**¹ ligands and two OH⁻ anions. The Co^{II} center is six coordinated by four N atoms from four independent **L**¹ ligands and two O atoms from OH⁻ anions to complete a distorted octahedral geometry with the coordination angles varying from 86.5(2)° to 179.7(4)°. The Co-O bond lengths are 2.069(4) Å, and the lengths of Co-N bonds are 2.128(6) Å and 2.130(6) Å, respectively. The equatorial plane is formed by four N atoms from four **L**¹ ligands, and the axial positions are occupied by two O atoms from two OH⁻ anions. All the **L**¹ ligands adopt monodentate coordination mode and two-coordinated OH⁻ anions not only participated in coordination but also are used to balance the charge.

As shown in Fig. 1b, such adjacent mononuclear structures are linked by O(1)-H(1A)···N(6) hydrogen bonds to form a one-dimensional chain [O(1)···N(6) separation is 2.781(8) Å, see Table 2 of Supplementary 1]. In addition, the C-H···N weak interactions are observed between adjacent chains. The distances of

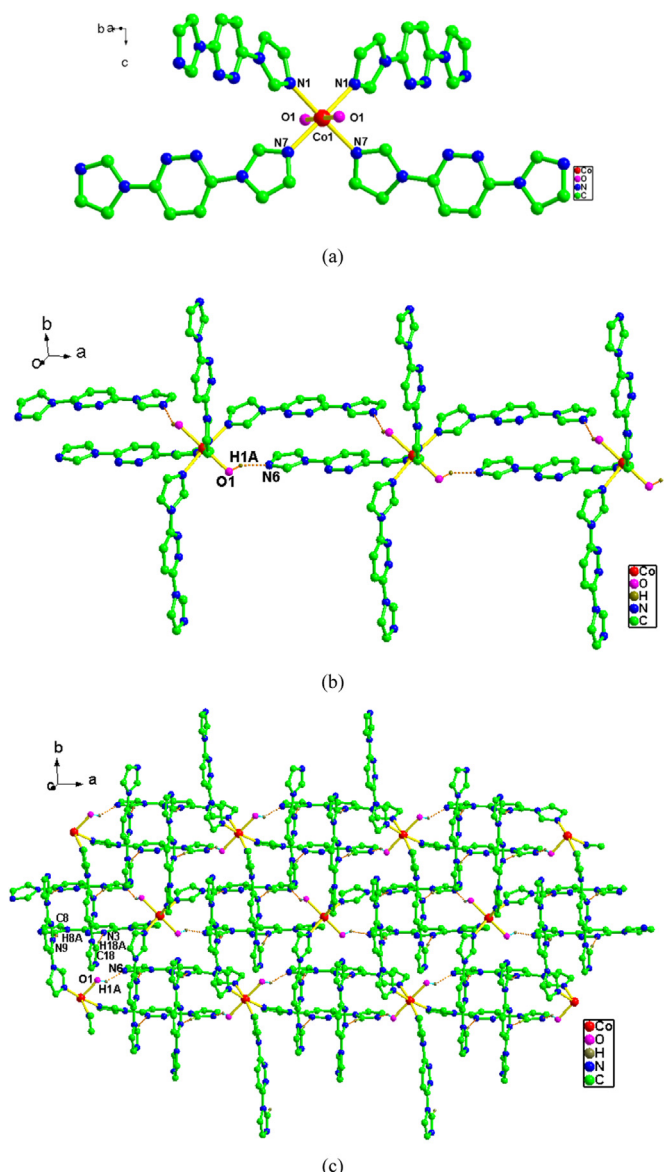


Fig. 1. View of (a) the coordination environment of Co^{II} ions in **1** (H atoms omitted for clarity) (b) the 1-D chain by the O–H...N hydrogen bonds of **1** (c) the 2-D supramolecular sheet formed by C–H...N weak interactions of **1**.

$\text{C}(8)\cdots\text{N}(9)$ and $\text{C}(18)\cdots\text{N}(3)$ are $3.416(5)$ and $3.415(4)$ Å, respectively. Therefore, such chains are further assembled by the C–H...N weak interactions between adjacent chains into an infinite 2-D supramolecular sheet (Fig. 1c).

3.2.2. $\{[\text{Co}(\text{L}^1)(\text{H}_2\text{O})_4] \cdot \text{ClO}_4\}_\infty(2)$

Single crystal X-ray diffraction analysis reveals that complex **2** crystallizes in the orthorhombic space group $C222(1)$. Complex **2** shows 1-D chain structure (Fig. 2a). The complex **2** contains one Co^{II} cation, two L^1 ligands, four coordinated H_2O molecules and two ClO_4^- anions. Obviously, the structural difference of **1** and **2** is attributable to the difference of coordination mode of ligand L^1 . The ligands L^1 in complex **2** adopt bidentate bridging mode coordinated to Co^{II} centers and extend to a 1-D chain. The Co^{II} ion possesses a slightly distorted (CoN_2O_4) octahedral configuration, which is coordinated by two N atoms originating from two distinct L^1 ligands [The $\text{Co}(1)\text{--N}(3)$ bond length is $2.155(7)$ Å] and four O atoms from four distinct H_2O molecules [The $\text{Co}(1)\text{--O}(1)$ bond length is $2.172(6)$ Å. $\text{Co}(1)\text{--O}(2)$ bond length is $2.069(7)$ Å]. The

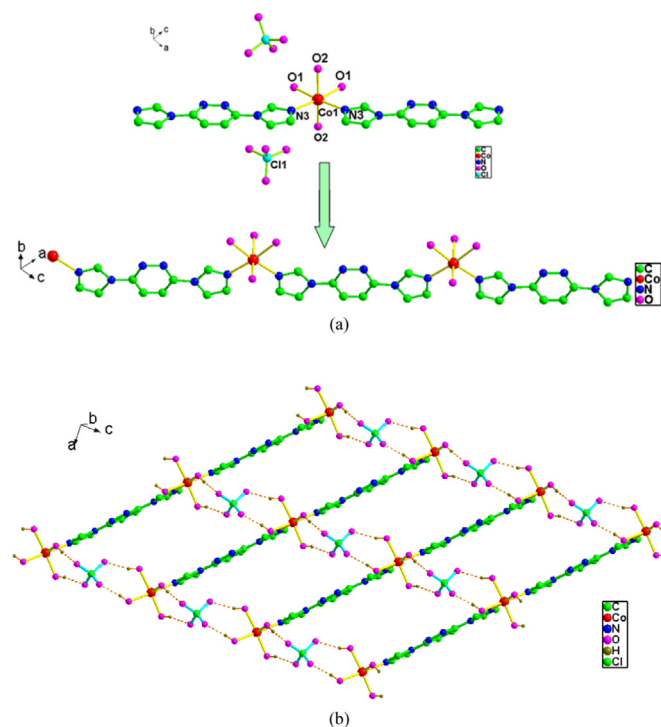


Fig. 2. View of the 1-D chain of **2** (H atoms omitted for clarity) (b) the 2-D supramolecular sheet formed O–H...O hydrogen-bonds.

neighboring non-bonding $\text{Co}\cdots\text{Co}$ distance is $12.9558(5)$ Å. Because of such coordination mode, the $[\text{CoL}^1(\text{H}_2\text{O})_4]^{2+}$ unit has two positive charge, the weaker coordination ability of ClO_4^- anion does not show any bonding interaction with Co^{II} , and only acts as counter anion for charge balance. The ClO_4^- anions are located in the cavities of the sheet and formed O–H...O hydrogen-bonding with the coordinated water molecules to develop a two-dimensional sheet [$\text{O}\cdots\text{O}$ separations are at the range of $2.718(8)$ – $2.792(9)$ Å] (Fig. 2b). The hydrogen-bonding parameters (Å, °) were listed in Table 2 of Supplementary 1.

3.2.3. $\{[\text{Co}(\text{L}^1)(\text{H}_2\text{O})_4] \cdot \text{SiF}_6\}_\infty(3)$

Complex **3** was obtained when the reaction of L^1 with $\text{CoSiF}_6 \cdot 6\text{H}_2\text{O}$ was carried out in the mixed solvent ($\text{H}_2\text{O}/\text{CH}_3\text{CH}_2\text{OH}$) at room temperature. Because of the weak coordination ability of SiF_6^{2-} anion, the 1-D chain structure of complex **3** was similar to **2** (Fig. 3a). But complex **3** crystallizes in the triclinic space group $P-1$. The Co^{II} center lies in a slightly distorted octahedral environment. Ligand L^1 acts as a typical bridging ligand coordinating to the Co^{II} ion, and the Co–N bond lengths are $2.110(5)$ and $2.114(5)$ Å, respectively. The N–Co–N angle is $98.3(2)^\circ$, which is smaller than that of **2**, so the neighboring non-bonding $\text{Co}\cdots\text{Co}$ distance (12.609 Å) connected by L^1 is shorter than that in complex **2**. Complex **3** as similar with **2**, SiF_6^{2-} anions do not show any bonding interactions with Co^{II} centers, and only act as counter anions for charge balance. The Co–O bond lengths are the range of $2.077(5)$ to $2.147(4)$ Å in complex **3**. It should be pointed out that N(5) and N(6) atoms of L^1 are not coordinated to Co^{II} ion, which present intermolecular O–H...N weak interaction with coordinated H_2O between the adjacent two chains [the $\text{O}(2)\cdots\text{N}(5)$ separation is $3.043(7)$ Å, the $\text{O}(3)\cdots\text{N}(6)$ separation is 3.066 Å] (Fig. 3b). Additionally, the uncoordinated SiF_6^{2-} anions serving as counter anions locate at the cavities of the sheets and form O–H...F hydrogen-bonding with the coordinated water molecules to give a three-dimensional framework [$\text{O}\cdots\text{F}$ separations are at the range of $2.637(7)$ – $3.146(10)$ Å, see also Table 2 of Supplementary 1] (Fig. 3c).

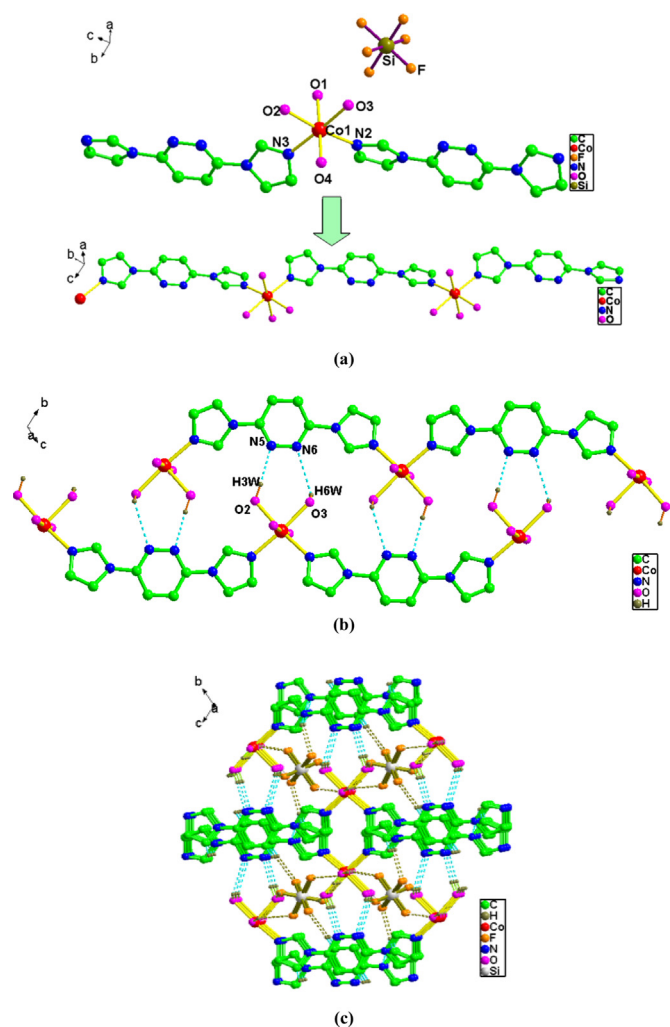


Fig. 3. View of (a) 1-D supramolecular chain of **3** (H atoms omitted for clarity) (b) the 1-D chain by the C-H...N weak interactions of **3** (c) the three-dimensional framework formed by O-H...F hydrogen-bonds of **3**.

3.2.4. $\{[Co(L^1)_3] \cdot 2ClO_4\}_\infty$ (**4**)

Complex **4** crystallizes in the trigonal space group $R\bar{3}c$. The complex **4** contains one crystallographically independent Co^{II} center and three L^1 ligands and two ClO_4^- anions. The X-ray diffraction analysis shows that complex **4** possesses 3-D network structure (Fig. 4b). The same metal salt and ligand L^1 were used to prepared complexes **2** and **4**, but obtained entirely different structures. The main reason is that the solvent was different. The Co^{II} center can be coordinated by six N atoms from six distinct L^1 ligands, which shows a slightly distorted octahedral geometry (Fig. 4a). The coordination angles around Co^{II} center are varying from $89.62(9)^\circ$ to $180.00(14)^\circ$, and the Co-N bond lengths are 2.162 (2) Å. In addition, the uncoordinated ClO_4^- anions were located in the voids in the 3-D framework structure in order to keeping the balance of charge instead of taking part in coordination (Fig. 4c). Meanwhile, considering the Co^{II} centers linked by the L^1 ligands, the 3-D framework of complex **4** can be rationalized to be a $\{412.63\}$ 6-c topological net with the stoichiometry uninodal net (Fig. 4d).

3.2.5. $[Co(L^2)Cl_2]_\infty$ (**5**)

Single crystal X-ray diffraction analysis reveals that complex **5** shows 1-D zigzag chain structure (Fig. 5). Complex **5** crystallizes in the orthorhombic space group $P2(1)2(1)2(1)$. The complex **5** contains one Co^{II} center, two neutral L^2 ligands and two Cl^- anions.

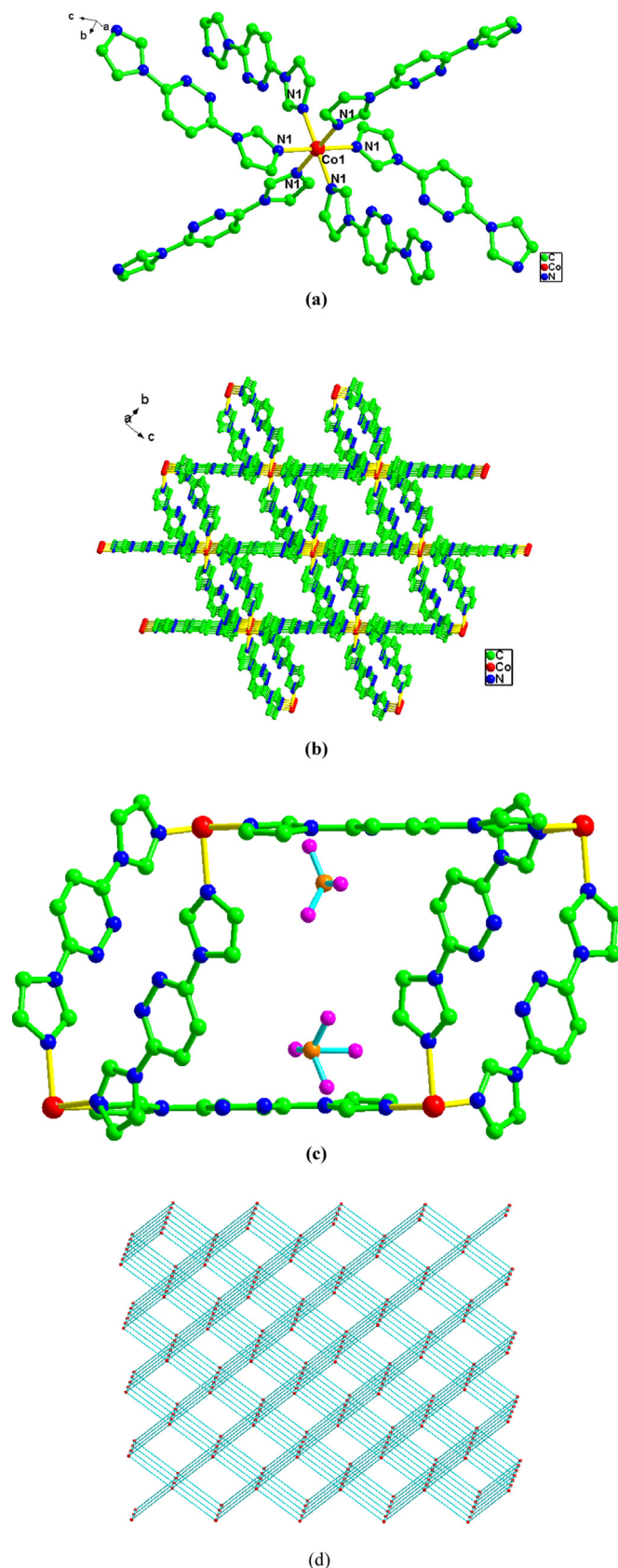


Fig. 4. View of (a) the coordination environment of Co^{II} ions in **4** (b) the 3-D network of **4** (c) the ClO_4^- anions in 3-D network of **4** (d) topological view of **4** (Co^{II} acts as sixconnected node, just a Co^{II} center linked by L^1 was considered) (H atoms omitted for clarity).

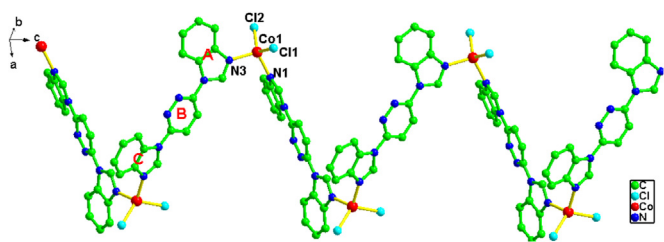


Fig. 5. View of the 1-D zigzag chain structure of **5** (H atoms omitted for clarity).

In complex **5**, the Co^{II} center adopts a distorted tetrahedral coordinated geometry coordinated to two N atoms from two distinct L² ligands and two Cl⁻ anions. The Co-N bond lengths are 2.021(3) and 2.031(3) Å, respectively. The Co(1)-Cl(1) bond length is 2.2279(12) Å, Co(1)-Cl(2) bond length is 2.2389(11) Å. The neighboring non-bonding Co...Co distance is 12.819(7) Å, which is shorter than the length of **2**, longer than that of **3**. In the 1-D zigzag chain, the angle of Co...Co...Co linked by the L² ligands is 71.620(4)°. The bond angle of N-Co-N is 105.59(14)°. The angles N-Co-Cl are ranging from 101.37(10)° to 114.11(10)°. The Cl⁻ anions not only take part in coordination but also serve as counter anions. All the L² ligands are equivalent in complex **5**. The pyridazine ring and two benzimidazole rings are not on the same plane in the one L² ligand. The both dihedral angles between planes A and B, C and B are 15.6°, the dihedral angle between planes A and C is 24.8° (Fig. 5).

3.2.6. $[\text{Co}(\text{L}^2)_2] \cdot \text{SiF}_6$ (**6**)

Complex **6** crystallizes in the tetragonal with space group P4 (2)/n. Complex **6** is a rhombohedral grid (Fig. 6b) with a (4, 4)

topology (Fig. 6c). The complex **6** contains a Co^{II} center, two neutral L² ligands, one uncoordinated SiF₆²⁻. Compared with complexes **1–4**, the Co^{II} centers adopt a distorted tetrahedral coordinated geometry in complexes **5** and **6**. The reason is that the steric hindrance of benzimidazole-ring is larger than that of imidazole-ring.

In complex **6**, the Co^{II} center is coordinated to four N atoms from four distinct L² ligands [The Co-N bond lengths are 1.996 (5) Å] to complete a distorted tetrahedral coordinated geometry and the coordination angles 108.50(7) and 111.43(15)°, respectively (Fig. 6a and Table 1 of Supplementary 1). Each L² ligand links two Co^{II} ions and in turn each Co^{II} ion connects four ligands forming a layer structure with (4, 4) foursquare grid units. Meanwhile, all the Co^{II} ions are located in one plane (Fig. 6b). From Fig. 6b, we can see that each (4, 4) grid unit is constructed by four ligands acting as four edges and four Co^{II} ions as four vertexs. All the lengths of the edges are equal (the edges are 12.574 Å) and the orthogonal distance is 17.782 Å. The uncoordinated SiF₆²⁻ anions serving as counter anions are located in the cavities of the sheets. In complex **6**, the both dihedral angles between planes A and B, C and B are 29.8°, while the dihedral angles between planes A and C are 59.6° (Fig. 6a). The two kinds of dihedral angles are larger than those in complex **5**.

3.3. Thermal stabilities and powder X-ray diffraction of the complexes

To examine the thermal stabilities of complexes **1–6**, the TGA analyses of complexes **1–6** were carried out from room temperature to 1000 °C at the rate of 10 °C·min⁻¹ in nitrogen atmosphere, as shown in Fig. S1 of Supplementary 2. The TGA study of

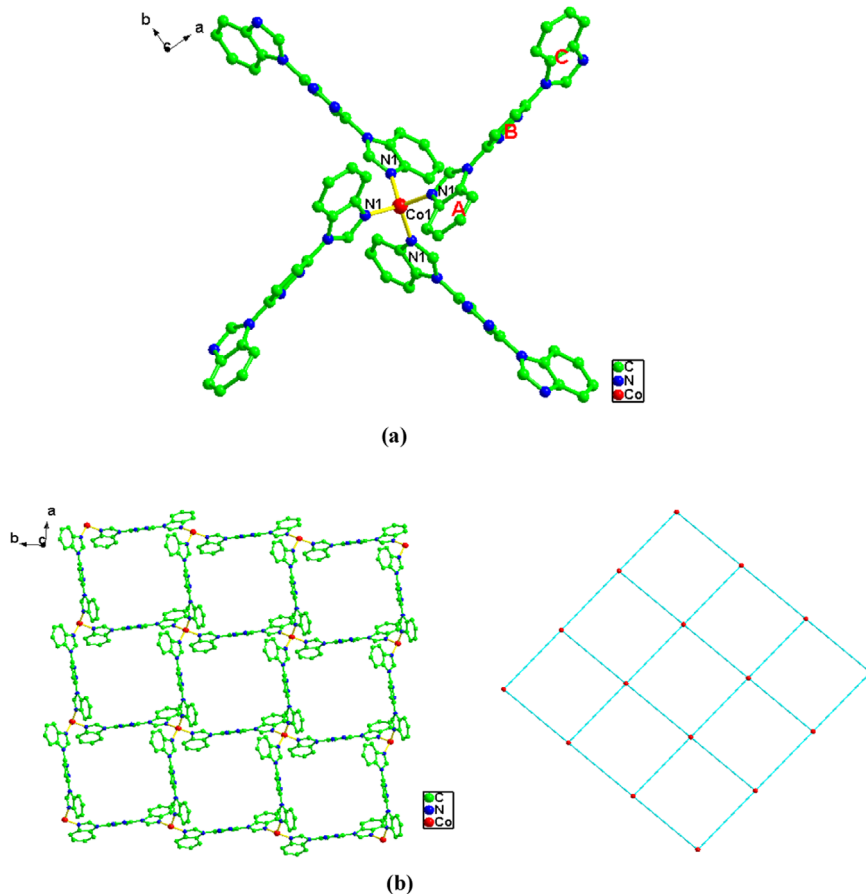


Fig. 6. View of (a) the coordination environment of Co^{II} ions in **6** (b) 2-D (4,4) network structure of **6** (H atoms omitted for clarity).

complexes **1–6**, the weight loss is observed owing to the direct decomposition of coordinated water molecule and organic ligands, and continues to lose weight up to 1000 °C, indicating the continuous expulsion of organic moieties even at the upper limit of the measurement range. The TGA curve indicates the weight loss of **1** can be divided into two steps. The first step shows a slow weight loss from 25 °C to 145 °C, then the removal of organic ligands occurs within the range of 255–975 °C. The TGA curve of **2** displays a weight loss of 15.36% (Calcd. 13.28%) in the range of 25–162 °C corresponded to the loss of four coordinated water molecules. A weight loss is observed, which can be attributed to the decomposing of the organic ligands from 162 °C to 984 °C. The TGA curve of complex **3** shows that **3** is stable up to 93 °C and above that loss of organic ligands is observed. The TGA curve of complex **4** shows that a fast weight loss from 50 °C to 830 °C. Complexes **5** and **6** lose weight at about 397 °C and 230 °C to 973 °C and 980 °C, respectively, which demonstrates that complexes **5** and **6** are stable up to 230 °C. So the thermal stabilities of complexes **5** and **6** are better than complexes **1–4**, which indicates their thermostabilities are enhanced by aromatic ring.

To confirm whether the crystal structures are truly representative of the bulk materials, X-ray powder diffraction (XRPD) experiments were carried out for complexes **1–6**. The XRPD experimental and computer-simulated patterns of the corresponding complexes are shown in Fig. S2 of Supplementary 2. Although the experimental patterns have a few unindexed diffraction lines and some are slightly broadened in comparison with those simulated from the single crystal modes. It still can be considered favorably that the bulk synthesized materials and the as-grown crystals were homogeneous for **1–6**.

3.4. Luminescent property of the complexes

The solid-state photoluminescence property of complexes **1–6** as well as the ligands **L¹** and **L²** were investigated at room temperature (Supplementary 3). The free ligand **L¹** exhibits blue fluorescent emission band at 403 nm upon excitation at 247 nm, which can be originated from ligand center electronic transitions, that is, the $n \rightarrow \pi^*$ or $\pi \rightarrow \pi^*$ transition in nature according to the reported literature [24]. Upon excitation with 250 nm light, complexes **1–4** display fluorescent emission bands at 403, 403, 406 and 395 nm, respectively. The results reveal that the peaks of the emission spectra for **1–3** are very close to that of the free ligand **L¹**, which can probably be attributed to the intraligand electronic transition [25]. The slightly blue shift of emission peak occurs in complex **4**, which is probably due to the coordination environment around Co^{II} center. Since the photoluminescence behavior is closely associated with the metal ions and the ligands coordinated around it [26].

The conjugate aromatic rings of **L²** are larger than that of **L¹**, so the ligand **L²** presented emission bands at 469 nm excited bands at 370 nm. Complexes **5** and **6** display fluorescent emission bands at 446 and 408 nm upon excitation at 370 and 250 nm, respectively. Complexes **5** and **6** reveal similar blue shifts of the emission peak, which also attributed to intraligand electronic transition [27] and decrease of planarity of **L²**. The decreased degree in **6** is larger than that in **5**. The luminescent differences between **5** and **6** may be probably assigned to the differences of coordination environment and the solvent molecules. The enhance of luminescence efficiency can be attributed to the ligand coordination to the metal center, which enhances the rigidity of the ligand and thus reduces the loss of energy through a radiationless pathway [28].

3.5. Photocatalytic activity

Most of the photocatalytic reactions taken place in the

heterogeneous system for purifying water by thoroughly decomposing organic pollutants [29]. In this work, we take the advantage of complexes **1–6** degrading methylene blue (MB), whose characteristic absorption band is 664 nm. The photocatalytic reactions were performed as follow process: 50 mg of the title complexes was dispersed in 50 mL aqueous solution of MB (10 mg · L⁻¹) under stirring in the dark for 30 min to ensure the equilibrium of the mixed solution. Then the mixed solution was exposed to UV irradiation from an Hg lamp (300W) and kept under continuous stirring during irradiations for 6 h. Samples of 4 mL were taken every 30 min for analysis. The final results show that the degradation rate (deduct the self-degradation) of MB is 25.1% for **1**, 16.8% for **2**, 28.5% for **4**, 15.4% for **5**, 10.1% for **6**. The curves of absorbance of the MB solution degraded by **1–6** of under UV light are shown Fig. S1 of Supplementary 4. The absorption spectra of the MB solution during the decomposition reaction under UV irradiation is shown Fig. S3 of Supplementary 4. When no catalyst was added, the degradation rate of MB is 54.8% within 6 h under UV irradiation. However, complex **3** can restrain the photodegradation of dyes. The results indicate that complexes **1**, **2** and **4–6** show photocatalytic activity for the degradation of MB. The photocatalytic activity of TiO₂ have been reported in literature [30]. Compared with TiO₂, the degradation ability of the complexes is weaker than that of TiO₂.

The possible photocatalytic mechanism for the above degradation reactions is proposed as follows, (Fig. S2 of Supplementary 4). Generally, the catalyst can be photo-activated by a photon with irradiation energy equal to or higher than its band gap energy (E_g), electrons (e⁻) in the valence band (VB) of title complexes are excited to the conduction band (CB) at the photocatalytic surface which generate same amount of holes (h⁺) in the VB. Then O₂ may be reduced into O₂⁻ by the combination of electrons (e⁻), which may further turn into hydroxyl radicals (·OH). Meanwhile, interaction of holes (h⁺) with hydroxyl (OH⁻) may generate the ·OH active radicals. As we all know, the ·OH active works as a strong oxidizing agent to decompose MB effectively and complete the photocatalytic process [31].

4. Conclusion

In conclusion, we have successfully synthesized and characterized a series of new Co^{II} complexes with two structurally related ligands, 3,6-bis(*N*-imidazolyl) pyridazine (**L¹**) and 3,6-bis(*N*-benzimidazolyl) pyridazine (**L²**). The influences of the structure of ligands on the resultant structures of Co^{II} complexes are briefly discussed. Some intra-molecular and/or inter-molecular weak interactions, such as hydrogen bonding, also play important role in the formation of these complexes, especially in the aspects of linking the discrete subunits and low-dimensional entities into high-dimensional supramolecular networks. Moreover, the fluorescence property of ligands **L¹**, **L²** and part of complexes display blue fluorescent emission at room temperature. The photocatalytic activity of complexes **1–6** proved that they may be photocatalysts for degradation of organic dyes in a certain extent. This approach may be useful for the construction of a variety of new Co^{II} metal complexes that have the potential of fluorescent or photocatalytic activity.

Acknowledgments

This work was financially supported by the National Natural Science Foundation of China (No. 21361026).

Appendix A. Supporting information

Supplementary data associated with this article can be found in the online version at <http://dx.doi.org/10.1016/j.jssc.2016.04.037>.

References

- [1] (a) X.J. Li, Z.J. Yu, T.N. Guan, X.X. Li, G.C. Ma, X.F. Guo, *Cryst. Growth Des.* 15 (2015) 278;
 (b) L.L. Zhang, J. Guo, Q.G. Meng, R.M. Wang, D.F. Sun, *CrystEngComm* 15 (2013) 9578;
 (c) B.Q. Song, C. Qin, Y.T. Zhang, X.S. Wu, H.S. Liu, K.Z. Shao, Z.M. Su, *CrystEngComm* 17 (2015) 3129;
 (d) L. Chen, G.J. Xu, K.Z. Shao, Y.H. Zhao, G.S. Yang, Y.Q. Lan, X.L. Wang, H.B. Xu, Z.M. Su, *CrystEngComm* 12 (2010) 2157.
- [2] (a) D.Q. Yuan, D. Zhao, D.F. Sun, H.C. Zhou, *Angew. Chem. Int. Ed.* 49 (2010) 5357;
 (b) D.F. Sun, S.Q. Ma, Y.X. Ke, D.J. Collins, H.C. Zhou, *J. Am. Chem. Soc.* 128 (2006) 3896;
 (c) S. Qiu, G. Zhu, *Coord. Chem. Rev.* 253 (2009) 2891;
 (d) H. Kim, G. Park, K. Kim, *CrystEngComm* 10 (2008) 954.
- [3] (a) Z. Liu, W. He, Z. Guo, *Chem. Soc. Rev.* 42 (2013) 1568;
 (b) H. Xu, R. Chen, Q. Sun, W. Lai, Q. Su, W. Huang, X. Liu, *Chem. Soc. Rev.* 43 (2014) 3259;
 (c) Q. Chen, Z. Chang, W.C. Song, H. Song, H.B. Song, T.L. Hu, X.H. Bu, *Angew. Chem. Int. Ed.* 52 (2013) 11550;
 (d) L.J. Murray, M. Dinc, J.R. Long, *Chem. Soc. Rev.* 38 (2009) 1294;
 (e) Y.Z. Zheng, G.J. Zhou, Z. Zheng, R.E.P. Winpenny, *Chem. Soc. Rev.* 43 (2014) 1462.
- [4] (a) R.J. Wei, Q. Huo, J. Tao, R.B. Huang, L.S. Zheng, *Angew. Chem. Int. Ed.* 50 (2011) 8940;
 (b) X.X. Li, H.Y. Xu, F.Z. Kong, R.H. Wang, *Angew. Chem. Int. Ed.* 52 (2013) 13769;
 (c) B.Y. Li, Y.M. Zhang, D.X. Ma, T.L. Ma, Z. Shi, S.Q. Ma, *J. Am. Chem. Soc.* 136 (2014) 1202.
- [5] (a) Z. Yan, M. Li, H.L. Gao, X.C. Huang, D. Li, *Chem. Commun.* 48 (2012) 3960;
 (b) H.X. Zhao, X.X. Li, J.Y. Wang, L.Y. Li, R.H. Wang, *ChemPlusChem* 78 (2013) 1491;
 (c) C.R. Murdock, B.C. Hughes, Z. Lu, D.M. Jenkins, *Coord. Chem. Rev.* 119 (2014) 258;
 (d) J.H. Wang, M. Li, D. Li, *Chem. Sci.* 4 (2013) 1793.
- [6] (a) X. Zhuang, Y. Wan, C. Feng, Y. Shen, D. Zhao, *Chem. Mater.* 21 (2009) 706;
 (b) M.L. Ma, J.H. Qin, C. Ji, H. Xu, R. Wang, B.J. Li, S.Q. Zang, H.W. Hou, S. R. Batten, *J. Mater. Chem. C* 12 (2014) 1085;
 (c) J. Tang, Y. Liu, H. Li, Z. Tan, D. Li, *Chem. Commun.* 49 (2013) 5498;
 (d) X.L. Wang, J. Luan, F.F. Sui, H.Y. Lin, G.C. Liu, C. Xu, *Cryst. Growth Des.* 13 (2013) 3561.
- [7] G.B. Li, J.R. He, M. Pan, H.Y. Deng, J.M. Liu, C.Y. Su, *Dalton Trans.* 41 (2012) 4626.
- [8] (a) Q.G. Meng, L.T. Wang, J.T. Lu, X. Wang, W. Lu, Z.Y. Song, *Aust. J. Chem.* 68 (2015) 742;
 (b) L.M. Fan, X.T. Zhang, Z. Sun, W. Zhang, Y.S. Ding, W.L. Fan, L.M. Sun, X. Zhao, H. Lei, *Cryst. Growth Des.* 13 (2013) 2462.
- [9] Y.J. Mu, G. Han, S.Y. Ji, H.W. Hou, Y.T. Fan, *CrystEngComm* 13 (2011) 5943.
- [10] (a) X.M. Chen, M.L. Tong, *Acc. Chem. Rev.* 40 (2007) 162;
 (b) J.R. Li, J. Sculley, H.C. Zhou, *Chem. Rev.* 112 (2012) 869;
 (c) L. Mihalcea, N. Henry, T. Bousquet, C. Volkringer, T. Loiseau, *Cryst. Growth Des.* 12 (2012) 4641;
 (d) C. Wei, C.K. Xia, Y.L. Wu, F. Wu, S. Yang, J.L. Ma, *Polyhedron* 89 (2015) 189.
- [11] (a) S.L. Li, Y.Q. Lan, J.C. Ma, J.F. Ma, Z.M. Su, *Cryst. Growth Des.* 10 (2010) 1161;
 (b) R. Risoluti, D. Piazzese, A. Napoli, S. Materazzi, *J. Anal. Appl. Pyrolysis* 117 (2016) 82;
 (c) M.E. Moghadam, A. Divsalar, A.A. Shahrnoy, A.A. Saboury, *J. Biomol. Struct. Dyn.* (2015) 1.
- [12] (a) X.X. Wang, Y.J. Ma, H.H. Li, G.H. Cui, *Transit. Met. Chem.* 40 (2015) 99;
 (b) C.Y. Xu, L.K. Li, Y.P. Wang, Q.Q. Guo, X.J. Wang, H.W. Hou, Y.T. Fan, *Cryst. Growth Des.* 11 (2011) 4667;
 (c) H. Jiang, Y.T. Liu, J.F. Ma, W.L. Zhang, J. Yang, *Polyhedron* 27 (2008) 2595;
 (d) L. Liu, Y.H. Liu, G. Han, D.Q. Wu, H.W. Hou, Y.T. Fan, *Inorg. Chim. Acta* 403 (2013) 25.
- [13] (a) Q.X. Yang, X.Q. Chen, J.H. Cui, J.S. Hu, M.D. Zhang, L. Qin, G.F. Wang, Q.Y. Lu, H.G. Zheng, *Cryst. Growth Des.* 12 (2012) 4072;
 (b) F.L. Hu, W. Wu, P. Liang, Y.Q. Gu, L.G. Zhu, H. Wei, J.P. Lang, *Cryst. Growth Des.* 13 (2013) 5050;
 (c) W.T. Yang, T. Tian, H.Y. Wu, Q.J. Pan, S. Dang, Z.M. Sun, *Inorg. Chem.* 52 (2013) 2736.
- [14] Y.Y. Yang, L. Xu, G.G. Gao, F.Y. Li, Y.F. Qiu, X.S. Qu, H. Liu, *Eur. J. Inorg. Chem.* (2007) 2500.
- [15] J. Liu, M. Qu, M. Rouzies, X.M. Zhang, R. Clerac, *Inorg. Chem.* 53 (2014) 7870.
- [16] Q. Gao, Y.M. Chen, Y.L. Liu, C. Li, D.D. Gao, B. Wu, H.Y. Li, W. Liu, W. Li, *J. Coord. Chem.* 67 (2014) 1673.
- [17] X.L. Wang, X.T. Sha, G.C. Liu, N.L. Chen, Y. Tian, *CrystEngComm* 17 (2015) 7290.
- [18] S. Brooker, *Eur. J. Inorg. Chem.* (2002) 2535.
- [19] U. Beckmann, S. Brooker, *Coord. Chem. Rev.* 245 (2003) 17.
- [20] S.W. Jin, D.Q. Wang, *J. Coord. Chem.* 63 (2010) 3042.
- [21] S.W. Jin, D.Q. Wang, *J. Coord. Chem.* 65 (2012) 1937.
- [22] AXS Bruker, *SAINT Software Reference Manual*, Madison, WI, (1998).
- [23] G.M. Sheldrick, *Acta Crystallogr. Sect. A: Found. Crystallogr.* 64 (2008) 112.
- [24] (a) K. Liu, B.H. Ma, X.L. Guo, D.X. Ma, L.K. Meng, G. Zeng, F. Yang, G.H. Li, Z. Shi, S.H. Feng, *CrystEngComm* 7 (2015) 5054;
 (b) X.Y. Wan, F.L. Jiang, L. Chen, J. Pan, K. Zhou, K.Z. Su, J.D. Pang, G.X. Lyuab, M. C. Hong, *CrystEngComm* 17 (2015) 3829.
- [25] (a) H. Wu, W. Dong, H.Y. Liu, J.F. Ma, S.L. Li, J. Yang, Y.Y. Liu, Z.M. Su, *Dalton Trans.* 39 (2008) 5331;
 (b) R.H. Wang, D.Q. Yuan, F.L. Jiang, L. Han, Y.Q. Gong, M.C. Hong, *Cryst. Growth Des.* 6 (2006) 1351.
- [26] L. Li, T.L. Hu, J.R. Li, D.Z. Wang, Y.F. Zeng, X.H. Bu, *CrystEngComm* 9 (2007) 411.
- [27] M.D. Zhang, L. Qin, H.T. Yang, Y.Z. Li, Z.J. Guo, H.G. Zheng, *Cryst. Growth Des.* 13 (2013) 1961.
- [28] (a) L.X. Cai, C. Chen, B. Tan, Y.J. Zhang, X.D. Yang, J. Zhang, *CrystEngComm* 17 (2015) 2353;
 (b) Z.R. Pan, H.G. Zheng, T.W. Wang, Y. Song, Y.Z. Li, Z.J. Guo, S.R. Batten, *Inorg. Chem.* 47 (2008) 9528.
- [29] (a) B. Liu, Z.T. Yu, J. Yang, W. Hua, Y.Y. Liu, J.F. Ma, *Inorg. Chem.* 50 (2011) 8967;
 (b) Y. Chen, N.P. Wang, C.P. Li, D.G. Wang, L. He, W. Li, Y.H. Li, J. Suo, *Mater. Focus* 4 (2015) 37;
 (c) Z.C. Shao, C. Huang, X. Han, H.R. Wang, A. Li, Y.B. Han, K. Li, H.W. Hou, Y. T. Fan, *Dalton Trans.* 44 (2015) 12832.
- [30] S.H. Wei, R. Wu, J.K. Jian, J. Hou, F.J. Chen, A. Ablata, Y.F. Sun, *RSC Adv.* 5 (2015) 40348.
- [31] J.Y. Zhang, Y.Y. Xing, Q.W. Wang, N. Zhang, W. Deng, E.Q. Gao, *J. Solid State Chem.* 232 (2015) 19.